3D Printed Terahertz Rectangular Waveguides of Polystyrene and TOPAS: a Comparison

Article *in* Journal of infrared, millimeter and terahertz waves · November 2018

DOI: 10.1007/s10762-018-0552-9

7 authors, including:

Rui Guo
Philipps University of Marburg
3 PUBLICATIONS **5** CITATIONS
SEE PROFILE

Felipe Beltran-Mejia
Instituto Nacional de Telecomunicações
31 PUBLICATIONS **99** CITATIONS
SEE PROFILE

Martin Koch
Philipps University of Marburg
660 PUBLICATIONS **11,732** CITATIONS
SEE PROFILE

Journal of Infrared, Millimeter, and Terahertz Waves
https://doi.org/10.1007/s10762-018-0552-9

3D Printed Terahertz Rectangular Waveguides of Polystyrene and TOPAS: a Comparison

R. Guo[1] · Eva-Maria Stuebling[1] · F. Beltran-Mejia[2] · D. Ulm[3] · T. Kleine-Ostmann[3] · F. Ehrig[4] · M. Koch[1]

Received: 28 September 2018 / Accepted: 1 November 2018/Published online: 13 November 2018

Terahertz (THz) technology is a rapidly developing field as THz systems hold a great potential for basic research, e.g., to study state-selective tunneling phenomena at individual molecules using a THz scanning tunneling microscope [1] or crystallization processes out of solution using a THz spectrometer [2]. Besides, real world applications such as industrial inspection [3, 4] or THz communications [5] are intensely discussed. A mature THz technology needs—besides sources and the detectors—devices to guide and manipulate THz waves. These not only include lenses, gratings, prisms, beam splitters, and polarizers but also waveguides and couplers. Recently, it was shown that 3D printing with polystyrene (PS) provides a fast and inexpensive method to produce such elements for the lower THz frequency range [6, 7]. Furthermore, PS provides a good compromise between low THz absorption and printability. However, it was shown that cyclic olefin copolymer—a material with very low THz absorption made by TOPAS—can be used to 3D print lenses and gratings, as well [8].

In this letter, we explore cyclic olefin copolymer (hereafter called TOPAS) for 3D printing of rectangular waveguides. Which, to the best of our knowledge, it is the first time a 3D printing technique is applied for the construction of a TOPAS THz waveguide. We also show that these TOPAS waveguides are superior to their PS counterpart. We attribute this to a more uniform arrangement of the deposited polymer layers, in particular due to the higher homogeneity of the lateral boundaries of the TOPAS waveguides in comparison to those made of PS.

✉ Eva-Maria Stuebling
eva-maria.stuebling@physik.uni-marburg.de

[1] Department of Physics, Philipps-Universität Marburg, Renthof 5, 35032 Marburg, Germany

[2] National Institute of Telecommunications – Inatel, Av. Joao Camargo 510, Santa Rita do Sapucai, MG 37540-000, Brazil

[3] Department High Frequency and Fields, Physikalisch-Technische Bundesanstalt (PTB), Bundesallee 100, 38116 Braunschweig, Germany

[4] IWK Institute of Material Science and Plastics Processing, Oberseestr. 10, 8640 Rapperswil, Switzerland

Previously, a micro structured polymer optical fiber (mPOF) was made out of TOPAS in [9] by using the stack and draw technique. Later, a Bragg grating recorded on a TOPAS mPOF was constructed by drilling and drawing a cylindrical preform. Unfortunately, using a drawing tower for prototyping THz waveguides is both expensive and time demanding. On the other hand, there are no commercial filaments for 3D printing with TOPAS. This may be due to the high stiffness of this material. For this reason, the filament used here was produced on a special double-strand extrusion line of the Institute of Material Science and Plastics Processing (IWK) in Switzerland.

Here, we demonstrate 3D printed TOPAS waveguides for the THz frequency range. All the waveguides were 3D printed using an Ultimaker3 with a maximum layer resolution (layer height) of 20 μm by using a nozzle size of 0.4 mm. The layer height can vary from 20 to 200 μm depending on the flow rate and the printing speed. The waveguides were printed with a layer resolution of 0.08 mm and a printing speed of 70 mm/s. They are characterized using an electronic 120-GHz emitter-receiver system [7]. Also, in order to guarantee single-mode propagation, all waveguides were designed with a $1.6 \times 1.6\text{-mm}^2$ cross section as explained in [7]. We used nozzle temperatures of 240 °C and 210 °C for PS and TOPAS, respectively, depending on the melting temperature of the two materials and their optimal adherence on the glass bed. The glass bed was heated up to 60 °C for both materials. In [7], it was determined that bending losses for 120 GHz were negligible for a curvature radius greater than 10 mm. For this reason, all waveguides had at least one 90° bend with a curvature radius equal to 20 mm to ensure the power measured at the receiver was solely confined radiation.

As shown in the insets of Fig. 1, seven waveguides with different lengths were printed for both materials, ranging from 91.4 to 427 mm. As shown, several bends were needed in order to be able to construct longer waveguides in one single print. Also, thin supporting flags were included in the design. These flags, which act as holders for the waveguides, are only 240 μm thick, so their influence on the guided radiation can be considered negligible.

A comparison between the 120-GHz properties of PS and TOPAS is presented in Table 1. The refractive index n and the material absorption α were measured using a quasi-optical system in the millimeter range described in [10]. For the measurement of the waveguide attenuation, we used the output intensity measurements at 120 GHz shown in Fig. 1. The propagation length l and the input P_0 and output power P follow the relation given by the Beer-Lambert law, $P=P_0 \cdot \exp(-\alpha \cdot l)$. Hence, it is possible to obtain the propagation loss for these

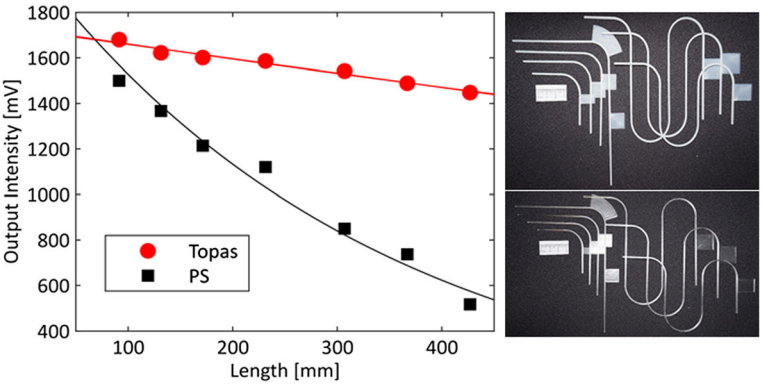

Fig. 1 Transmission measurements at 120 GHz for TOPAS and PS, red dots and black squares respectively. The curves represent nonlinear fits. On the right, pictures of the printed waveguides used during these measurements

Table 1 Optical parameters measured for polystyrene and TOPAS

@120 GHz	PS	TOPAS
Refractive index, n	1.574 ± 0.010	1.470 ± 0.021
Absorption coefficient, α (cm^{-1})	0.0003 ± 0.0005	0.0019 ± 0.00019
Attenuation (cm^{-1})	0.3	0.04

waveguides by fitting this expression with the measured data as it is represented by the curves in Fig. 1. The resulting values for the attenuation are at the bottom line of Table 1. The attenuation in the waveguides is much higher than concluded from the material absorption coefficient. This is mainly due to the wave propagation principle inside the waveguide which is based on multiple total reflections but also due to scattering losses in the printed waveguides the structure of which is not perfect but exhibits inhomogeneities. However, the attenuation in the TOPAS waveguides is smaller than in PS waveguides having the same dimension.

In order to understand why the attenuation coefficient is lower for TOPAS, although its bulk absorption coefficient is higher, it is important to consider the 3D printing process. This printer uses the fused deposition modeling technology, which consists on the deposition of stacked layers of thermoplastic. These layers are not homogeneous, mainly due to the different adhesive surface conditions of the first layer in comparison with the others. Besides, there are burrs at the ends of the waveguides caused by mechanical boundary conditions. As a result, the stacked layers exhibit some inhomogeneities that will lead to scattering and, hence, clearly affect the wave guiding properties. A typical cross section of one of these waveguides is shown

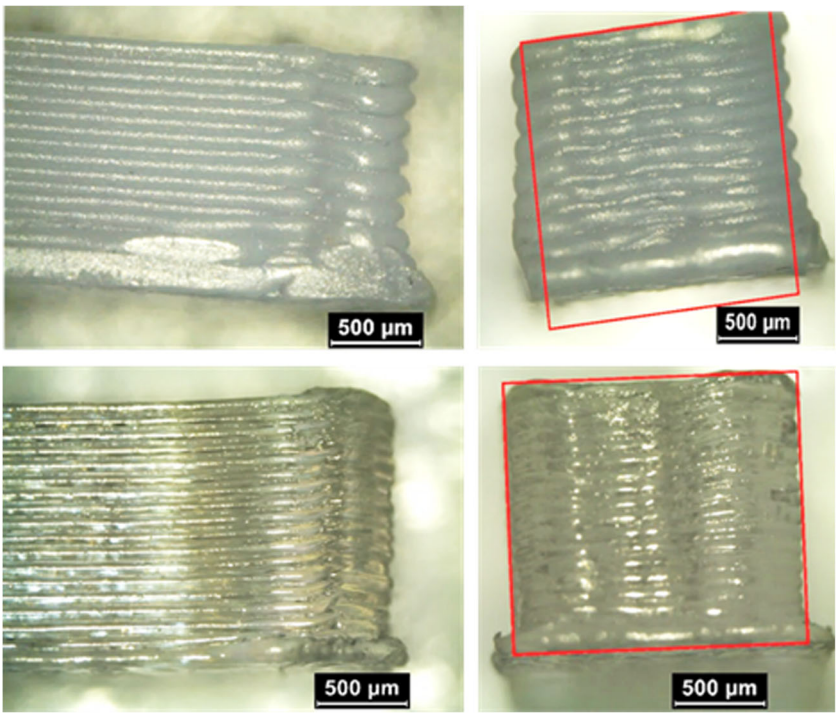

Fig. 2 Pictures of the lateral view (left) and the cross section (right) for polystyrene (top) and TOPAS (bottom) taken with a × 32 optical microscope. The red boxes at the left show the expected 1.6 × 1.6-mm^2 cross section

by the microscopic images presented in Fig. 2. For both materials, the printer was configured to deposit layers with a height of 0.08 mm. For the case of PS, the final result was different from the expected 1.6 × 1.6-mm^2 cross section as shown by the red rectangle on top of Fig. 2. The measured area of the cross section of a typical PS waveguide was about 1.75×1.50 mm^2 as measured with a vernier caliper. Therefore, the printed waveguide was lower and wider than what it was expected. In the same way, the lateral view and the cross section of a TOPAS waveguide are shown at the bottom of Fig. 2. The printed cross section, on the other hand, was closer to the expected dimensions. For this case, the measured cross section was approximately 0.2 mm wider than the expected cross section and it has smaller burrs than the PS counterpart. This lower surface roughness also explains the difference of the waveguide losses between the TOPAS and the PS waveguides.

In conclusion, TOPAS is a better material than PS for making waveguides for THz frequencies as shown by Fig. 1. This is not obvious, since the absorption coefficient of TOPAS is higher in comparison to PS at 120 GHz, as shown in Table 1. But also the mechanical properties of both materials play an important role in the homogeneity of the waveguide and the surface roughness on the boundaries. Finally, we have shown that it is also possible to 3D print high-quality and longer waveguides than what was previously possible by using home-made extruders for fabricating TOPAS filaments.

Funding Information F. Beltran-Mejia received funding from the Finep/Funttel (01.14.0231.00) under the Radiocommunication Reference Center—CRR, project of the National Institute of Telecommunications—Inatel, Brazil.

References

1. T. L. Cocker, D. Peller, P. Yu, J. Repp, and R. Huber, "Tracking the ultrafast motion of a single molecule by femtosecond orbital imaging," *Nature*, vol. 539, pp. 263–267, 2016.
2. A. Soltani, D. Gebauer, L. Duschek, B.M. Fischer, H. Cölfen, and M. Koch, "Crystallization Caught in the Act with Terahertz Spectroscopy: Non-Classical Pathway for l-(+)-Tartaric Acid," *Chemistry*, vol. 23, pp. 14128–14132, 2017.
3. S. Hunsche, M. Koch, I. Brener, and M. C. Nuss, "THz near-field imaging," *Opt Commun*, vol. 150, pp. 22–26, 1998.
4. I. Amenabar, F. Lopez, and A. Mendikute, "In Introductory Review to THz Non-Destructive Testing of Composite Mater," *J Infrared Millim Terahertz Waves*, vol. 34, pp. 152–169, 2013.
5. A. Kazemipour, M. Hudlička, R. Dickhoff, M. Salhi, T. Kleine-Ostmann, and T. Schrader, "The Horn Antenna as Gaussian Source in the mm-Wave Domain," *J Infrared Millim Terahertz Waves*, vol. 35, pp. 720–731, 2014.
6. S. F. Busch, M. Weidenbach, M. Fey, F. Schäfer, T. Probst, and M. Koch, "Optical Properties of 3D Printable Plastics in the THz Regime and their Application for 3D Printed THz Optics," *J Infrared Millim Terahertz Waves*, vol. 35, pp. 993–997, 2014.
7. M. Weidenbach, D. Jahn, A. Rehn, S.F. Busch, F. Beltrán-Mejía, J.C. Balzer, and M. Koch, "3D printed dielectric rectangular waveguides, splitters and couplers for 120 GHz," *Opt. Express,* vol. 24, pp. 28968–28976, 2016.
8. S. F. Busch, M. Weidenbach, J. C. Balzer, and M. Koch, "THz Optics 3D Printed with TOPAS," *J Infrared Millim Terahertz Waves*, vol. 37, pp. 303–307, 2016.
9. K. Nielsen, H. K. Rasmussen, A. J. L. Adam, P. C. M. Planken, O. Bang, and P. U. Jepsen, "Bendable, low-loss Topas fibers for the terahertz frequency range," *Opt. Express*, vol. 17, pp. 8592–8601, 2009.
10. A. Kazemipour, M. Hudlicka, S.-K. Yee, M.A. Salhi, D. Allal, T. Kleine-Ostmann, and T. Schrader, "Design and calibration of a compact quasi-optical system for material characterization in millimeter/submillimeter wave domain," *IEEE Trans Instrum Meas*, vol. 64, pp. 1438–1445, 2015.